Compact Modeling of Intrinsic Capacitances in AlGaN/GaN HEMT Devices

Sourabh Khandelwal* and Tor A. Fjeldly

Dept. of Electronics and Telecommunications, Norwegian University of Science and Technology Trondheim, Norway, *sourabh.khandelwal@ntnu.no

ABSTRACT

We present an analytical model for intrinsic gate-source and gate-drain capacitances in AlGaN/GaN HEMT devices. A physics-based analytical expression for 2-DEG charge density developed previously by our group along with the Meyer capacitance formulations is used to derive the intrinsic capacitances. The model is in excellent agreement with experimental data.

Keywords: AlGaN/GaN HEMTs, MODFETs, Compact Models

1 INTRODUCTION

AlGaN/GaN HEMT devices are being actively pursued for high power and high frequency applications [1-2] in industry and academia, owing to their excellent characteristics like high breakdown voltage, high charge density, and high electron mobility [3-5]. To explore and exploit the full potential of these devices, accurate and fast simulation of circuits based on these devices is required. The speed and accuracy of such simulations depend heavily on the compact model used to describe behavior of the device, which underlines the importance of an analytical physics-based model for these devices.

To the best of the authors' knowledge, currently available models for these devices are primarily based on numerical calculations, semi-empirical model expressions, and/or simplifying approximations [6-11]. Models relying on numerical calculations will be slow because of the iterative nature. Semi-empirical models are fast but do not provide needed insight into the device operation. They also tend to have a large number of empirical parameters, which have to be extracted from experimental data. In contrast to these approaches, we present a physics based analytical model for intrinsic capacitances in these devices with a minimal parameter set.

An analytical physics-based expression for 2-DEG charge density n_s developed previously by our group is used to derive the gate-channel capacitance C_{ch} valid in all the regions of device operation. We use the developed C_{ch} model in conjunction with the Meyer capacitance model to derive continuous expressions for intrinsic gate-source and gate-drain capacitances valid in all the regions of device operation. With long channel approximation all the nine trans-capacitances in the device can be obtained from the present model.

The paper is arranged as follows. In section 2, we present the details of the model for intrinsic capacitances. The developed model is verified by comparing with experimental data in section 3. In section 4, we conclude the paper.

2 MODEL DESCRIPTION

A cross-sectional view of the AlGaN/GaN HEMT device discussed here is shown in Fig. 1. The equations derived in this work are for the channel region under the gate contact. The source-gate and drain-gate gap regions are treated as parasitic resistances.

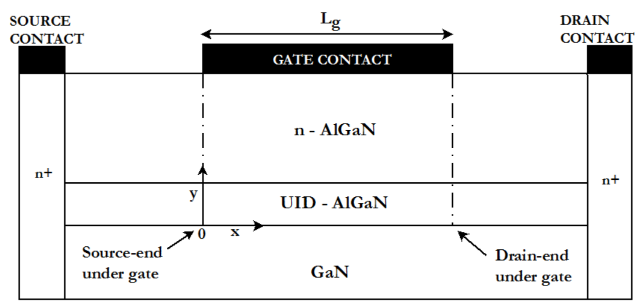

Figure 1. Cross sectional view (not drawn to scale) of AlGaN/GaN HEMT. UID is a thin un-intentionally doped AlGaN layer commonly used for mobility enhancement.

The 2-DEG charge density is one of the principal entities governing the performance and operation of AlGaN/GaN HEMT devices. It can be calculated from the solution of Schrodinger's and Poisson's equations in the quantum well assuming a triangular potential profile. A self-consistent solution of n_s considering the two important energy levels is expressed as [7],

$$n_s = DV_{th}\left\{\ln\left[\exp\left(\frac{E_f - E_0}{V_{th}}\right)+1\right]+\ln\left[\exp\left(\frac{E_f - E_1}{V_{th}}\right)+1\right]\right\} \quad (1)$$

$$E_0 = \gamma_0 n_s^{2/3}, E_1 = \gamma_1 n_s^{2/3} \quad (2)$$

$$n_s = \frac{\varepsilon}{qd}\left(V_{go} - E_f - V_x\right) \quad (3)$$

where $V_{go} = V_g - V_{off}$ and V_x is the potential at any point x in the channel. A description of all the other symbols used is

Symbol	Physical meaning
V_{th}	Thermal Voltage
D	Thickness of AlGaN layer
q	The electron charge
ε	The permittivity of AlGaN
D	Density of States
V_{off}	Cut-off voltage
V_{go}	V_g-V_{off}
E_0	Position of first sub-band
E_1	Position of second sub-band
E_f	Position of Fermi level
C_g	ε/d AlGaN layer Capacitance
γ_0,γ_1	Experimentally determined parameters

Table 1. List of symbols used.

given in Table 1. It is apparent that to obtain an analytical solution from (1) – (3), we need to make simplifications. This is done by subdividing the variation of n_s versus the applied gate voltage into different operating regions, allowing us to derive explicit expression in each one. This subdivision is determined by the position of the Fermi level E_f relative to the energy levels E_0 and E_1. The regional analytical solutions are then combined to provide a continuous model for n_s valid across all the regions.

The various regions of the subdivision are identified in Fig. 2, together with the numerical solution for E_f, E_0 and E_1 versus V_g. The regions are: (i) $V_g < V_{off}$, the sub-V_{off} region, where $|E_f|$ is comparable to $|V_{go}|$; (ii) $V_g > V_{off}$, and $E_f < E_0$, the moderate 2-DEG region ; (iii) $V_g > V_{off}$ and $E_f > E_0$, the strong 2-DEG region. In the sub-V_{off} region, $|E_f| >> E_0$ and E_1 (see Fig. 2) and therefore $E_f - E_0$ and $E_f - E_1 \approx E_f$. Applying this observation and using the approximation $\ln(1 + x) \approx x$ for $x << 1$ to (1), and invoking (3), the solution for n_s can be written in terms of a Lambert's function as,

$$\frac{qn_s}{C_gV_{th}}\exp\left(\frac{qn_s}{C_gV_{th}}\right)=\frac{2qD}{C_g}\exp\left(\frac{V_{go}}{V_{th}}\right) \quad (4)$$

Performing a Taylor series expansion of (4) and neglecting higher order terms, we obtain the following explicit function for n_s in the sub-V_{off} region,

$$n_{s,sub-V_{off}}=2DV_{th}\exp\left(\frac{V_{go}}{V_{th}}\right) \quad (5)$$

This expression is valid when $|E_f| >> E_0$, E_1 and $E_f < 0$.

The model for n_s valid in the moderate 2-DEG and strong 2-DEG regions can be written as [12],

$$n_{s,above-V_{off}}=\frac{C_gV_{go}}{q}H(V_{go}) \quad (6)$$

where

$$H(V_{go})=\frac{V_{go}+V_{th}\left[1-\ln(\beta V_{gon})\right]-\frac{\gamma_0}{3}\left(\frac{C_gV_{go}}{q}\right)^{2/3}}{V_{go}\left(1+\frac{V_{th}}{V_{god}}\right)+\frac{2\gamma_0}{3}\left(\frac{C_gV_{go}}{q}\right)^{2/3}} \quad (7)$$

Here, V_{gon} and V_{god} are functions of V_{go} given by the interpolation expression,

$$V_{gox}=\frac{V_{go}\alpha_x}{\sqrt{V_{go}^2+\alpha_x^2}} \quad (8)$$

and $\beta = C_g / qDV_{th}$, $\alpha_n = e/\beta$ and $\alpha_d = 1/\beta$.

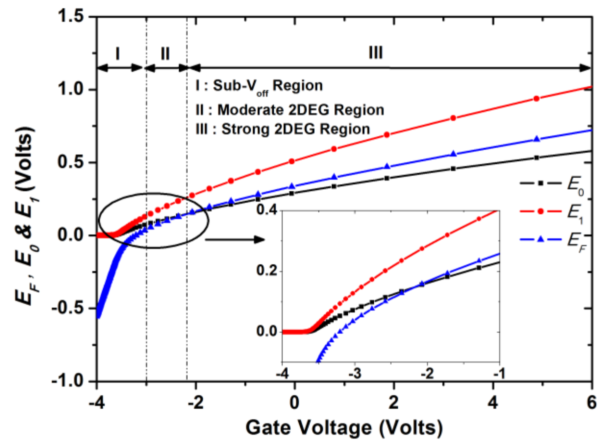

Figure 2. Numerical solution of E_f, E_0 and E_1 with the gate voltage. Typical V_{off} = -3 V used. The regions identified for developing analytical solution are marked in the figure.

For the purpose of developing a compact model, a continuous unified expression for n_s valid in all regions of operation is desirable. This is possible by combining (5) – (7) in the following manner,

$$n_{s,unified}=\frac{2V_{th}(C_g/q)\ln\{1+\exp(V_{go}/2V_{th})\}}{1/H(V_{go})+(C_g/qD)\exp(-V_{go}/2V_{th})} \quad (9)$$

From this expression we readily observe that (6) is recovered when $V_g > V_{off}$, and (5) results in the sub-V_{off} region. Hence (9) describes the variation of the 2-DEG charge density with the applied voltage in all the regions of operation.

The material system in HEMT devices is metal-AlGaN-GaN. For a useful operating range the Schottky junction (metal-AlGaN) is reverse biased and the AlGaN layer is fully depleted. This makes the system a non-linear capacitor as only displacement current is expected. The displacement current is due to the variation in the 2-DEG and the GaN layer charge with V_g. When the 2-DEG is strong, it shields the GaN layer charge, and C_g in such a case is equal to the gate-channel capacitance C_{ch}, which is qdn_s/dV_g. The expression for C_{ch} is obtained as,

$$C_{ch} = 2V_{th}C_g \left\{ \frac{\frac{V'_{ge}}{V_{ge}}\left(G\left(V_{go}\right) + \beta V_{th}(V_{ge}-1)\right)}{\left(G\left(V_{go}\right) + \beta V_{th}(V_{-ge}-1)\right)^2} \right\} - \quad (10)$$

$$2V_{th}C_g \left\{ \frac{\ln(V_{ge})\left(G'\left(V_{go}\right) + \beta V_{th}V'_{-ge}\right)}{\left(G\left(V_{go}\right) + \beta V_{th}(V_{-ge}-1)\right)^2} \right\}$$

where $V_{ge} = 1 + e^{V_{go}/2V_{th}}$, $V_{-ge} = 1 + e^{-V_{go}/2V_{th}}$, $V_{ge}' = \frac{dV_{ge}}{dV_g}$, $V_{-ge}' = \frac{dV_{-ge}}{dV_g}$ and $G(V_{go}) = 1/H(V_{go})$.

Using the C_{ch} model in conjunction with the Meyer capacitance model [13], we obtain the following continuous expressions for the intrinsic gate-drain and gate-source capacitances per unit area covering all regimes of operation,

$$C_{gs} = \frac{2}{3}C_{ch}\left[1 - \left(\frac{V_{goe} - V_{dse}}{2V_{goe} - V_{dse}}\right)^2\right] \quad (11)$$

and

$$C_{gd} = \frac{2}{3}C_{ch}\left[1 - \left(\frac{V_{goe}}{2V_{goe} - V_{dse}}\right)^2\right] \quad (12)$$

Here V_{goe} is the effective gate overdrive voltage, which is equal to V_{go} above V_{off} and is of the order of the thermal voltage in the sub-V_{off} region. The expression used to model this behavior is,

$$V_{goe} = V_{th}\left\{1 + \frac{V_{go}}{2V_{th}} + \sqrt{\Delta^2 + \left(\frac{V_{go}}{2V_{th}} - 1\right)^2}\right\} \quad (13)$$

where Δ determines the width of transition region. V_{dse} in (11) and (12) is the effective drain-source voltage which is equal to V_{ds} for $V_{ds} < V_{goe}$ and V_{goe} for $V_{ds} > V_{goe}$. This behavior is modeled using,

$$V_{dse} = \frac{1}{2}\left[V_{ds} + V_{goe} - \sqrt{V_{\Delta}^{\ 2} + \left(V_{ds} - V_{goe}\right)^2}\right] \quad (14)$$

where V_{Δ} is determines the width of transition region for V_{dse}. Taking the long-channel approximation with $C_{ds} = C_{sd} \approx 0$, it is possible to obtain all the 9 non-reciprocal intrinsic device capacitances using the present model along with following relations [14],

$$C_{dd} = C_{dg} + C_{ds} = C_{sd} + C_{gd} \quad (15)$$

$$C_{ss} = C_{sg} + C_{sd} = C_{ds} + C_{gs} \quad (16)$$

$$C_{gg} = C_{gs} + C_{gd} = C_{sg} + C_{dg} \quad (17)$$

3 RESULTS AND DISCUSSIONS

The capacitance model presented in the previous section is correlated with experimental data for gate-source and gate-drain capacitances for a device with channel length 0.35 μm from [11]. In Fig. 3, we show the comparison between the model and experimental data for C_{gs}. The cut-off voltage for this device is -2.8 V. When V_g is below V_{off}, the 2-DEG charge density is very small and the capacitance is mainly due to fringing field. The value of the fringe capacitance is found to be 0.37 pF/mm. When V_g goes above but close to V_{off}, the 2-DEG charge density rapidly increases with V_g causing the observed rise in C_{gs}. For Vg well above V_{off} the 2-DEG charge density becomes close to a linear function of V_g causing the saturation of C_{gs}. It is apparent from Fig. 3 that the model captures all the regions of device operation quite well.

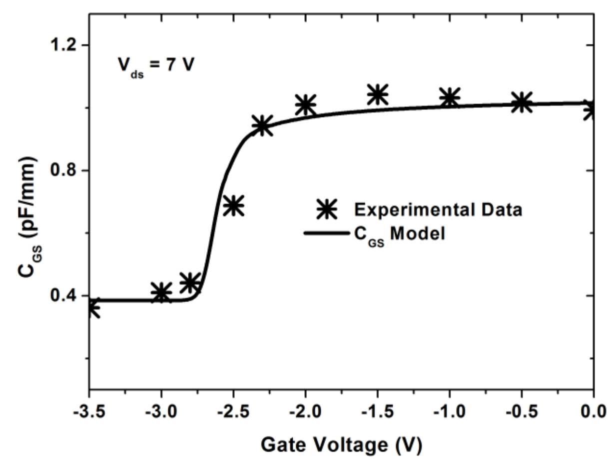

Figure 3. Comparison of modeled C_{gs} Vs V_{gs} with experimental data for 0.35 μm channel length device. Experimental data is taken from [11].

In Fig. 4, we compare the model with experimental data for C_{gd} versus V_{ds}. A steady decrease in C_{gd} with V_{ds} is apparent from Fig. 4, which indicates that the drain loses control of the channel charge. This happens because increasing the drain voltage after saturation only moves the point of saturation slightly without causing substantial change to the charge in the channel. An excellent correlation between the model and experimental data verified the developed modeling methodology.

4 CONCLUSIONS

We have presented an analytical physics-based model for intrinsic capacitances in AlGaN/GaN HEMT devices. An analytical 2-DEG charge density model valid in all the regions of device operation is used to derive gate-channel

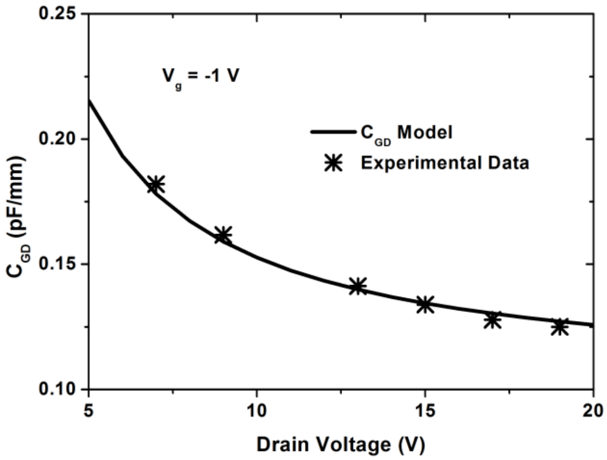

Figure 4. Comparison of modeled C_{gd} Vs V_{ds} with experimental data for 0.35 µm channel length device. Experimental data is taken from [11].

capacitance model. The gate-channel capacitance model is used in conjunction of Meyer capacitance model to derive the intrinsic capacitances in AlGaN/GaN HEMT devices. The model is in excellent agreement with experimental data. The proposed model can serve as basis for development of a complete compact model for AlGaN/GaN HEMT devices.

5 ACKNOWLEDGEMENTS

The work was carried out with support by the European Commission under Grant Agreement 218255 (COMON), and the Norwegian Research Council under contract 970141669 (MUSIC).

REFERENCES

[1] U. K. Mishra, L. Shen, T. E. Kazior, and Yi-Feng Wu, “GaN-Based RF power devices and amplifiers” *Proc. IEEE*, vol.96, no.2, pp.287-305, Feb. 2008.

[2] Y. Okamoto, A. Wakejima, Y. Ando, T. Yakanama, K. Matsunaga, and H. Miyamoto, “100W C-band single chip GaN FET power amplifier”, *Electronics Lett*., vol. 42, no. 5, pp. 283-285, March 2006.

[3] R. T. Kemberley, H. B. Wallace, and M. N. Yoder, “Impact of wide bandgap microwave devices on DoD systems”, *Proc. IEEE*, vol. 90, pp. 1059-1064, June 2002.

[4] L. M. Tolbert, B. Ozpineci, S. K. Islam, and M. S. Chinthavali, “Wide band-gap semiconductors for utility applications”, *Proc. Power and Energy System*. ACTA Press, USA, Feb. 2003

[5] R. J. Trew, “SiC and GaN transistors – Is there one winner for microwave power applications?,” *Proc. IEEE*, vol. 90, pp. 1032-1047, June 2002.

[6] X. Cheng and Y. Wang., “A Surface-Potential-Based Compact Model for AlGaN/GaN MODFETs,” *IEEE Trans. Electron Devices*, vol. 58, pp. 448-454, February 2011.

[7] S. Kola, J. M. Golio, and G. N. Maracas “An analytical expression for Fermi Level versus sheet carrier concentration for HEMT modeling”, *IEEE Electron device Lett.*, vol. 9, pp. 136-138, March 1988.

[8] I. Angelov, H. Zirath, and N. Rorsman “A new empirical non-linear model for HEMT and MESFET devices” *International Trans. on Microwave Theory and Techniques* vol. 40, no. 12, pp. 2258-2266, Dec. 1992.

[9] K. Lee, M. Shur, T. J. Drummond, and H. Morkoc, “Current-voltage and Capacitance-voltage Characteristics of Modulation Doped Field Transistors,” *IEEE Trans. Electron Devices*, vol. ED-30, no. 3, pp. 207-212, March 1983.

[10] Miao Li and Yan Wang, “2-D Analytical model for current-voltage characteristics and transconductance of AlGaN/GaN MODFETs” *IEEE Trans. Electron Devices*, vol. 55, no. 1, pp. 261-267, Jan. 2008.

[11] X. Cheng, M. Li and Y. Wang, “Physics based compact model for AlGaN/GaN MODFET with closed form I-V and C-V characteristics” *IEEE Trans. Electron Devices*, vol. 56, no. 12, pp. 2881-2887, Dec. 2009.

[12] S. Khandelwal, N. Goyal, and T. A. Fjeldly, “A physics-based analytical model for 2-DEG charge density in AlGaN/GaN HEMT devices” *IEEE Trans. on Electron devices*, vol. 58, no. 10, Oct. 2011

[13] J. E. Meyer, “MOS Models and circuit simulations”, *RCA Rev.*, vol. 32, pp. 42-63, 1971.

[14] Operation and modeling of the MOS transistor, Y. Tsividis, Oxford University Press.